

Development of an integrated geophysical and hydrological approach to study
submarine groundwater discharge into the Forge River

A Final Report Presented

by

Jonathan Wanlass

to

The Graduate School

In Partial Fulfillment of the

Requirements

for the Degree of

Master of Science

in

Geosciences

with concentration in Hydrogeology

Stony Brook University

August 2009

Stony Brook University

The Graduate School

Jonathan Scott Wanlass

We, the Final Report committee for the above candidate for the
Master of Science in Geosciences with concentration in Hydrogeology degree,
Hereby recommend acceptance of this Final Report.

Teng-fong Wong, Research Advisor, Professor,
Department of Geosciences

Daniel Davis, Deputy Chairperson, Professor
Department of Geosciences

Gilbert Hanson, Distinguished Service Professor
Department of Geosciences

ACKNOWLEDGMENTS

I would like to thank Ronald Paulsen, Ralph Milito, Frank Basile and Louis Velasquez of the Suffolk County Department of Health Services, Office of Water Resources for their help during this project. I would also like to thank Neal Stark at the Cornell University Cooperative Extension of Suffolk County for his help in the field and the preparation of this report. I would also like to acknowledge the help received from Teng-fong Wong at Stony Brook University, Geosciences Department.

Abstract of the
Development of an integrated geophysical and hydrological approach to study submarine
groundwater discharge into the Forge River

By

Jonathan Scott Wanlass

Master of Science

in

Geosciences

with concentration in Hydrogeology

Stony Brook University

2009

This study was undertaken to determine the spatial and temporal distribution of SGD at selected sites along Forge River, using a multidisciplinary approach employing three complementary techniques. The *Trident* Probe is a direct-push system that integrates a temperature probe, an electrical conductivity probe, and a water sampler. Contrasts in temperature and conductivity between surface water and groundwater can be used to locate likely areas of groundwater impingement at depth. Stationary DC resistivity surveys were conducted using an Advanced Geosciences Inc. (AGI) *SuperSting* eight channel receiver, interfaced to a 112 foot cable with 56 electrodes at a spacing of two feet. The Ultrasonic Groundwater Seepage system is a seepage meter system for quantifying specific discharge rates from groundwater flow to coastal waters. Traditional seepage technology was modified and improved to include continuous flow detection with ultrasonic flow meters. The data collected showed similar results when comparing the different techniques. All of the approaches were able to recognize areas of SGD and some were able to quantify those findings. The *SuperSting* was used during a tidal cycle to determine if SGD rates are affected by tidal fluctuations. The results showed the increased movement of SGD through the underlying sediments during the period of a high to low tide. The increased SGD movement indicates that tidal fluctuations play a major role in the discharge rate of submarine groundwater. This study also showed that by using a multidisciplinary approach for determining SGD we are able to definitively map areas of high and low SGD rates.

TABLE OF CONTENTS

1	INTRODUCTION.....	1
2	DATA COLLECTION METHODS.....	5
	2.1 TRIDENT PROBE.....	6
	2.2 SUPERSTING™ AUTOMATIC RESISTIVITY AND EARTHIMAGER 2D.....	8
	2.3 ULTRASONIC GROUNDWATER SEEPAGE SYSTEM.....	10
	2.4 CLUSTER WELL AND CORE SAMPLING.....	11
3	RESULTS.....	13
	3.1 TRIDENT CONDUCTIVITY AND TEMPERATURE MAPPING.....	16
	3.2 SUPERSTING AUTOMATIC RESISTIVITY AND EARTHIMAGER 2D.....	20
	3.3 ULTRASONIC GROUNDWATER SEEPAGE MEASUREMENTS.....	21
	3.4 CLUSTER-WELL SURVEY RESULTS.....	30
	3.5 CORE SAMPLING RESULTS.....	32
4	CONCLUSIONS.....	34
5	REFERENCES.....	37

LIST OF FIGURES

Figure 1-1. Site investigation location map with reference.....	3
Figure 2-1. Complete Trident probe showing sensor, water sampling probes, push-pole, GPS, and deck unit.....	7
Figure 2-2. SuperSting control box and electrode cable.....	9
Figure 2-3. Resistivity meter deployment technique.....	10
Figure 2-4. Ultrasonic seepage funnels, meters and buoy system.....	11
Figure 2-5. SCDHS pontoon vessel with AMS PowerProbe.....	12
Figure 3-1. Residential density survey.....	14
Figure 3-2. Site map showing Trident survey locations.....	16
Figure 3-3. Site map showing Trident conductivity results for transect FR-2.....	17
Figure 3-4. Site map showing Trident temperature results for transect FR-2.....	19
Figure 3-5. SuperSting profile of submarine sediments across transect fr-2 with approximate well-cluster locations and depth.....	20
Figure 3-6. Resistivity plot showing little SGD during high tide.....	21
Figure 3-7. Resistivity plot showing increased SGD during low tide.....	21
Figure 3-8. Site map showing Ultrasonic Seepage meter deployment locations.....	22
Figure 3-9. Ultrasonic seepage flow data for funnel 1 at station FR2-A.....	23
Figure 3-10. Ultrasonic seepage flow data for funnel 2 at station FR2-A.....	24
Figure 3-11. Ultrasonic seepage flow data for funnel 1 at station FR2-B.....	26
Figure 3-12. Ultrasonic seepage flow data for funnel 1 at station FR2-D.....	28
Figure 3-13. Ultrasonic seepage flow data for funnel 2 at station FR2-D.....	29
Figure 3-14. Site map showing locations of cluster wells.....	30
Figure 3-15. Site map showing locations of sediment core sampling.....	32

LIST OF TABLES

Table 3-1. Water quality results for the shoreline wells.....	15
Table 3-2. Trident results for the Forge River transect FR-2.....	16
Table 3-3. Results of cluster well sampling.....	31
Table 3-4. Core sample classification for transect FR-2.....	33

1 INTRODUCTION

The Forge River is located between the hamlets of Moriches and Mastic on the southwestern portion of Suffolk County in New York State (Figure 1-1). As a major tributary of Moriches Bay on the south shore of Long Island, it has been an important and productive natural resource for both commercial and recreational users for many decades. Since 2005 the Forge River has experienced chronic hypoxia due to excessive nitrogen input from a number of natural and anthropogenic sources, including storm water discharges, submarine discharges that contain effluent from unsewered high-density residential housing, and wastewater from a commercial duck farm upstream. These events have triggered concerns over the health of the River, the most alarming of which was a fish-kill during the summer of 2006. As a result of this particular event and documented evidence of a general decline in its state of health, Forge River was added to the 2006 New York State 303(d) List of Impaired Water Bodies.

Management and ecological restoration of the Forge River watershed hinge upon a comprehensive understanding of where and how nutrient loading is occurring. As is typical of Long Island streams, a significant portion of the freshwater flow of Forge River derives from groundwater, which may transport a disproportionate concentration of nutrients from the underground aquifer by submarine groundwater discharge (SGD). In a recent study of benthic fluxes of Forge River, *Aller et al.* [2009] observed that the groundwater fluxes are relatively high, representing up to 73% of the total external supply of nitrogen. As this flux is largest on the more densely populated western side of the Forge watershed, it has probably contributed to the greater hypoxia and nitrogen, as well as lower oxygen levels observed in the tributaries and shorelines along the western portions of the Forge River.

In relation to this issue, it is important to characterize the SGD and its spatial distribution along the Forge River. In addition, SGD is expected to vary over time, especially in connection with the tidal cycles. The tidal portion of Forge River is approximately three miles long, encompassing four branches off its main stem on the west side and two on the east side. Tidal loading can exert significant influence over the encroachment of saltwater from the ocean that is counteracted by underground underflow driven by the hydraulic gradient of the aquifer. The temporal evolution of SGD is such that its peak occurs near low tide and vice versa [*Paulsen et al.*, 2001; *Taniguchi*, 2002].



Figure 1-1. Site investigation location map with reference.

This study was undertaken to determine the spatial and temporal distribution of SGD at selected sites along Forge River, using a multidisciplinary approach employing three complementary techniques. In the past decade, significant advances in the technology of seepage meter for quantifying SGD have contributed to the acquisition of data of relatively high quality in many parts of the world [Zektser *et al.*, 2006]. The first approach we used is the direct measurement of seepage by an ultrasonic meter developed by *Paulsen et al.* [2001], which has the capability to measure both positive and reverse SGD with a resolution of $0.1 \mu\text{m/s}$ (0.086 cm/d). The time resolution is sufficiently refined that the evolution of SGD in response to tidal loading can be captured. This seepage meter is also robust enough for deployment in the field for over one month [Paulsen *et al.*, 2004].

A general observation in a coastal setting is that SGD rates differ significantly

between the off-shore and near-shore environments. Typically the discharge rate is the highest just landward of the saltwater-freshwater interface, and decays as one moves offshore towards the ocean [Bokuniewicz and Zeitlin, 1980; Taniguchi *et al.*, 2006]. Although the ultrasonic seepage meter provides data of high quality, it has an intrinsic limitation in that the spatial coverage is localized and it cannot conveniently map out the spatial heterogeneity of SGD over a relatively large area. In recent years there has been an increased use of electrical resistivity methods in hydrogeologic investigations, since they can provide extensive spatial coverage and in the context of a coastal setting, the electrical resistivity of the sediments provides a proxy for SGD [Day-Lewis *et al.*, 2006]. Electrical resistivity data acquired by a linear array on the surface can be inverted to derive the 2-dimensional resistivity profile of a vertical cross-section. Since the electrical resistivity of a porous medium is primarily controlled by its porosity and the electrical resistivity of the electrolyte in the pore space [Telford *et al.*, 1990], the inferred electrical resistivity at a given point on the vertical section can be related to the electrolyte resistivity if the sediment porosity is relatively uniform in the section. In particular, a relatively high electrical resistivity would imply a relatively low salinity, probably due to the influx of SGD [Swarzenski *et al.*, 2007]. If repeated measurements during a tidal cycle were able to resolve changes in the spatial distribution of electrical conductivity, then the data can be inverted to infer the temporal evolution of SGD related to tidal fluctuation.

Since the interpretation of electrical resistivity data depends solely on inversion of surface measurements, it is important to validate the inferred values by conducting direct measurements of conductivity at depth. In this study this is achieved by our third approach using the Trident probe [Chadwick *et al.*, 2003], which measures the bulk electrical conductivity and subsurface temperature at selected locations. We will synthesize the three types of measurements, and compare them to water chemistry data that were collected from monitoring wells installed beneath the river bottom.

2 DATA COLLECTION METHODS

2.1 TRIDENT PROBE

The *Trident* Probe (Figure 2-1) is a direct-push system that integrates a temperature probe, an electrical conductivity probe, and a water sampler [Chadwick *et al.*, 2003]. Contrasts in temperature and conductivity between surface water and groundwater can be used to locate likely areas of groundwater impingement at depth. The water-sampling device is then used to collect samples for detailed chemical characterization of contaminants. The two probes and sampler are collocated in a triangular pattern with a spacing of about 11 inches on an aluminum mounting base. A push-pole is used to drive this assembly into the sediment to a selected depth. The head of the push-pole is fitted with a GPS unit with WAAS capability. Data from this GPS unit and the two probes are fed to a data logger, which provides real-time measurement of the temperature and conductivity of the porous sediment as functions the spatial coordinates.

The temperature sensor housed in titanium has a measurement range of -5 to +35 °C at an accuracy of 0.001 °C, and a resolution of 0.001 °C. Areas of groundwater seepage may appear either as warm or cold contrast to the surface water, depending on the seasonal and site characteristics.

The electrical conductivity probe utilizes a Wenner-type configuration, with two pairs of stainless steel electrodes. The pairs of electrodes are coupled through an underwater connector and cable to a control unit, which applies a known current between the outer electrode pair while monitoring the voltage between the inner pair of electrodes. The probe measures the electrical conductivity of the porous medium saturated with fluid in a volume that encloses the electrode array, which is a function of primarily the salinity, and secondarily of clay content and porosity. Areas of SGD originating from a terrestrial origin are generally associated with low conductivity.

The water-sampling unit can extract interstitial water from the sediment at selected depths down to about three feet below the sediment water interface. The porewater is extracted by a low-flow peristaltic pump through Teflon tubing (inside diameter 1/16 inch) that is housed in a stainless steel casing fitted with a solid tip (Figure 2-1). On the side of the casing near the tip there is an inlet port consisting of a slot covered by a small mesh size (241 µm) stainless steel screen.

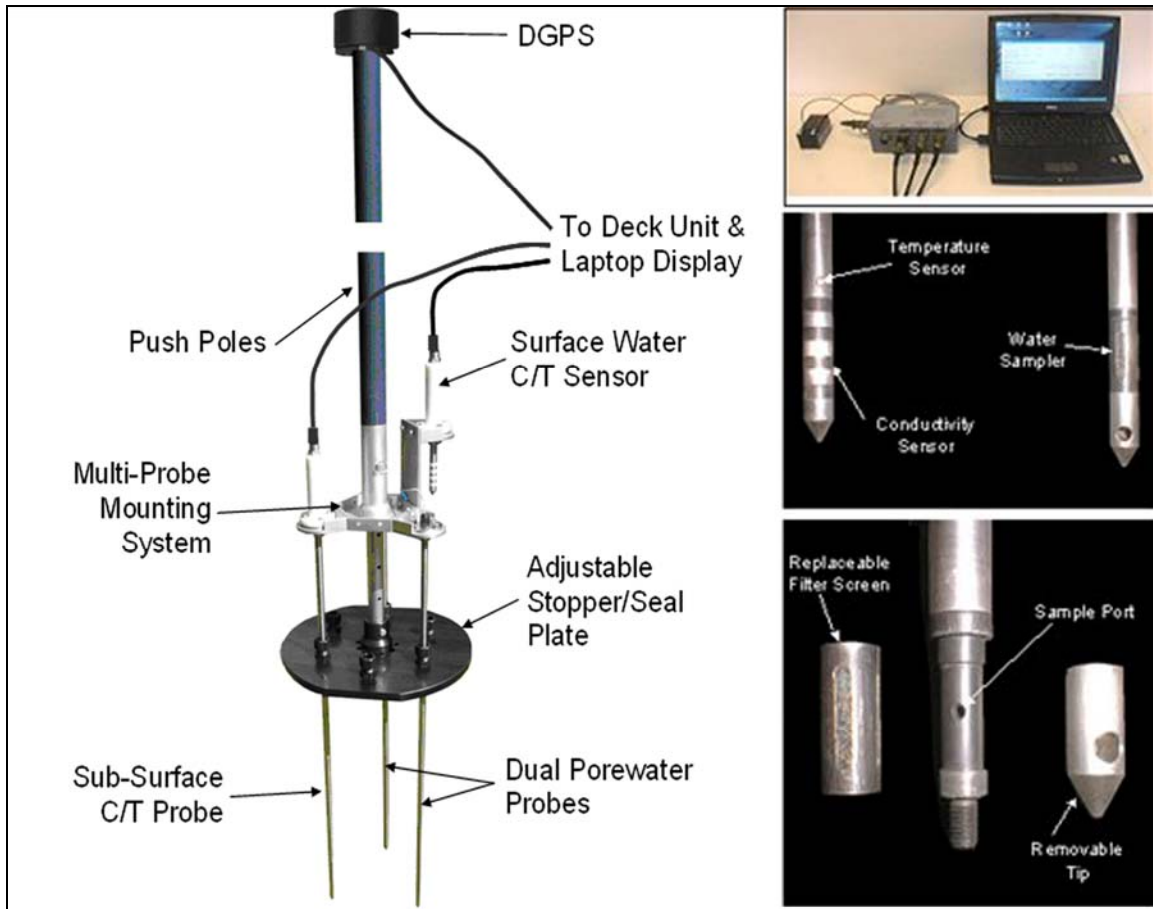


Figure 2-1. Complete Trident Probe system showing sensors, water sampling probes, push-pole, GPS and Deck unit.

The water-sampling system was first purged by pumping and discharging approximately 60 ml (estimated to be three times the volume of fluid in the system assuming a tubing 30 foot long). A volume of 250 ml was then extracted and stored in high-density polyethylene screw cap bottles for standard inorganics and dissolved metals analysis. Water quality analysis was also conducted *in situ* using a Myron UltraMeter 6P water quality analyzer (for temperature, conductivity, and pH) and a YSI 550 hand-held dissolved oxygen probe. The Myron UltraMeter's measurement range for temperature, conductivity and pH are 0 to +71 °C, 0 to 200 mS, and 0-14 pH. The accuracies are $\pm 1\%$, ± 0.01 pH, and ± 0.01 °C. The resolutions are 0.01, ± 0.01 pH, and 0.01 °C. The YSI 550 has a measurement range of 0 to 50 mg/L, a resolution of 0.01 mg/L and an accuracy of ± 0.3 mg/L. The water samples were unfiltered, but care was taken during the extraction process to minimize the amount of

suspended solids in the samples. Between stations, the screen zone was cleaned and the tubing replaced. The entire sampling system was then flushed with a series of solutions including surface seawater and deionized water.

In this study all the Trident measurements were made when the probes had been inserted to a depth of 1.5 feet below the sediment surface using the push-pole system. If the Trident push met with strong resistance at a depth less than the target depth of 1.5 feet, due to geological conditions or other obstructions, the station would be relocated laterally by a distance of approximately 1-2 feet, and the push repeated. Occasionally it was necessary to repeat the process up to three times to arrive at a location for a successful push. There were also instances when the sediments were so silty that the pumping system was unable to extract water samples. In these cases the station was relocated by a lateral distance of approximately 3-4 feet, and the push was repeated.

2.2 SUPERSTINGTM AUTOMATIC RESISTIVITY AND EARTHIMAGER 2D

Stationary DC resistivity surveys were conducted using an Advanced Geosciences Inc. (AGI) *SuperSting* eight channel receiver, interfaced to a 112 foot cable with 56 electrodes at a spacing of two feet (Figure 2-2). The cable with electrodes rested on top of the sediment, and the electrical resistivity was measured by distributed dipole-dipole and Schlumberger arrays to maximize resolution and the signal to noise ratio. The apparent resistivity values were processed with AGI's EarthImager 2D inversion and modeling software, using a homogeneous starting model and constrained by an underwater terrain file (that fixed the resistivity value of all grid points above the set cable depth at all iterations). The fixed resistivity value was determined by our data on the sea water using the Myron Ultrameter 6P, and the water depth profile was acquired by a Speedtech portable depth sounder capable of measuring 2 to 260 feet at a frequency of 200 kHz. Inversion parameters were set to AGI's default values for smooth inversion; the criteria for removal for low value resistivity data was 0.03 ohm-m; the damping factors were set to 10; the horizontal/vertical roughness ratio was set to 0.5; the resolution factor was set to 0.2; and the minimum allowed resistivity of 0.1 ohm-m.

To obtain a complete profile across the Forge River, the first transect was made with the electrode cable on the west side extending perpendicular to the shore. It would take 47 minutes to complete the data acquisition process, after which the cable was moved by a lateral distance of 83 feet towards the east for the next transect measurement. A total of 9 transects (lasting 8 hours) were conducted, and their inverted profiles were stacked to derive a vertical profile (with a rectangular section ~800 ft wide and ~27 ft deep) across the river. In some locations where initial results indicated significant SGD, the cable would be deployed at the same transect locations while the surveys were repeated throughout the course of a tidal cycle. The inverted data on temporal evolution of electrical resistivity provide a useful proxy for the transient development of SGD during a tidal cycle.



Figure 2-2. SuperSting control box and electrode cable

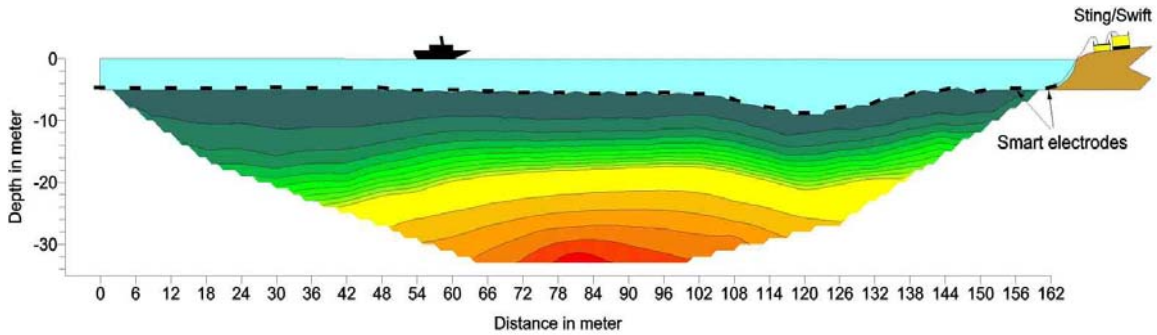


Figure 2-3. Resistivity meter deployment technique

2.3 ULTRASONIC GROUNDWATER SEEPAGE SYSTEM

The Ultrasonic Groundwater Seepage system is a seepage meter system for quantifying specific discharge rates from groundwater flow to coastal waters (Figure 2-4). Traditional seepage technology was modified and improved to include continuous flow detection with ultrasonic flow meters [Paulsen *et.al.*, 2001]. Groundwater flow is captured and directed through a stainless steel funnel with a square cross section of 2.3 ft² that are inserted approximately four inches into the sediment and connected to the ultrasonic device by Tygon tubing. The ultrasonic meter houses two piezoelectric transducers mounted at opposite ends of a cylindrical flow tube. The transducers continually generate bursts of ultrasonic signals from one end to the other. Arrival of the ultrasonic signals is continuously monitored by the piezoelectric transducers and corrected for temperature and conductivity. In a static fluid, the sound speed is sensitively dependent on temperature and salinity. If the fluid flows with a velocity then travel time for the upstream propagation of sound waves against the flow direction is prolonged relative to that for downstream propagation. The ultrasonic seepage meters are able to measure SGD at rates as low as 0.1 $\mu\text{m}/\text{sec}$. The full explanation of the technology is described in detail in Paulsen *et al.* 2001. The data is stored internally in a logger as it is being collected and downloaded at the end of the sampling period. The data produced are time series, over tidal cycles of specific discharge. This allows an accurate determination of the presence or absence of TSGD into a bay or estuary. A positive measurement indicates SGD (falling tide) while a negative measurement indicates

bank storage which usually occurs during a rising tide. For this study the measurement durations consisted of a 24 hour period. The results of the *Trident* temperature and conductivity surveys that revealed major areas of SGD were used in order to determine the locations the Ultrasonic Groundwater Seepage Meters were deployed.

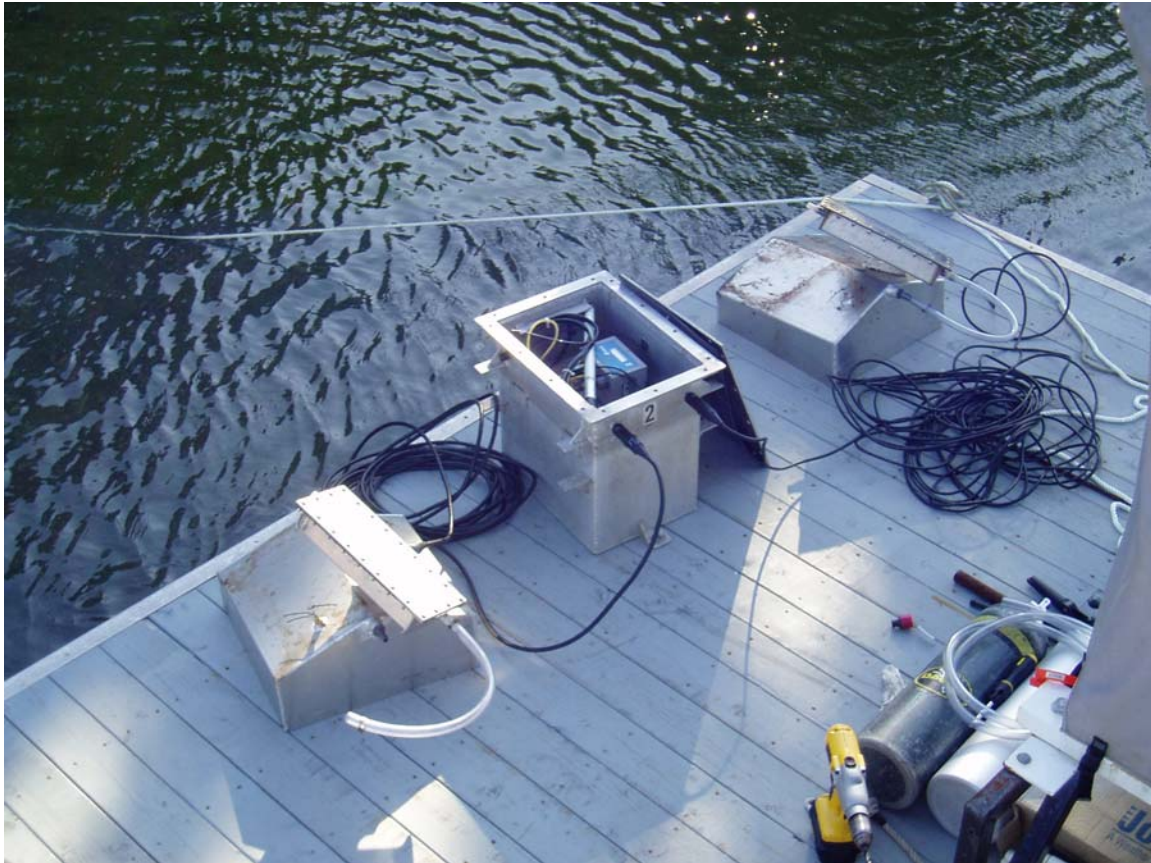


Figure 2-4. Ultrasonic seepage funnels, meters and buoy system.

2.4 CLUSTER WELL AND CORE SAMPLING

In addition to the technologies described above, groundwater sampling and submarine sediment profiling was achieved through a more traditional approach. Submarine cluster well installation and sediment core sampling were performed using a deck mounted AMS Power Probe on a thirty-two foot pontoon boat (Figure 2-5). Cluster wells were driven to various depths of from 1-2 feet to 9-10 feet below grade at six locations along transect FR-2. Prior to sampling, all sampling components were pre-cleaned in accordance with the Suffolk County Public and Environmental Health Laboratory protocols. The system was purged by first

pumping and discharging approximately three well volumes. Samples for standard inorganics and dissolved metals analysis were both collected in 250 ml natural high density polyethylene screw cap bottles. Water was also collected for water quality analysis using the Myron UltraMeter 6P water quality analyzer (temperature, conductivity, and pH) and a YSI 550 hand-held dissolved oxygen probe. The Myron UltraMeter's measurement range for temperature, conductivity and pH are 0 to +71 °C, 0 to 200 mS, and 0-14 pH. The accuracies are $\pm 1\%$, ± 0.01 pH, and ± 0.01 °C. The resolutions are 0.01, ± 0.01 pH, and 0.01 °C. The YSI 550 has a measurement range of 0 to 50 mg/L, a resolution of 0.01 mg/L and an accuracy of ± 0.3 mg/L. All samples were unfiltered. Care was taken during the pumping process to minimize the amount of suspended solids in the samples.

Core samples were taken at various depths below the silt layer. Each four-foot core sample was retrieved in a clear plastic tube, capped on the top and bottom, labeled and archived. Cross sections of the sediment layers were collected at selected locations where *Trident* results indicated potential SGD.



Figure 2-5. SCDHS pontoon vessel with AMS PowerProbe.

3 RESULTS

Recent studies have shown that the majority of the nitrogen input entering the Lower Forge River comes from SGD. Because of this fact, a residential density survey was conducted to determine the best location for the study area (Figure 3-1). Areas 1 and 5 show the highest density population (< 0.25 acre and 0.25-0.50 acre lot sizes), but area 5 is a gated community that has a sewage treatment plant which limits the nitrogen input to a specific location; therefore it was decided that area 1 was the best location.

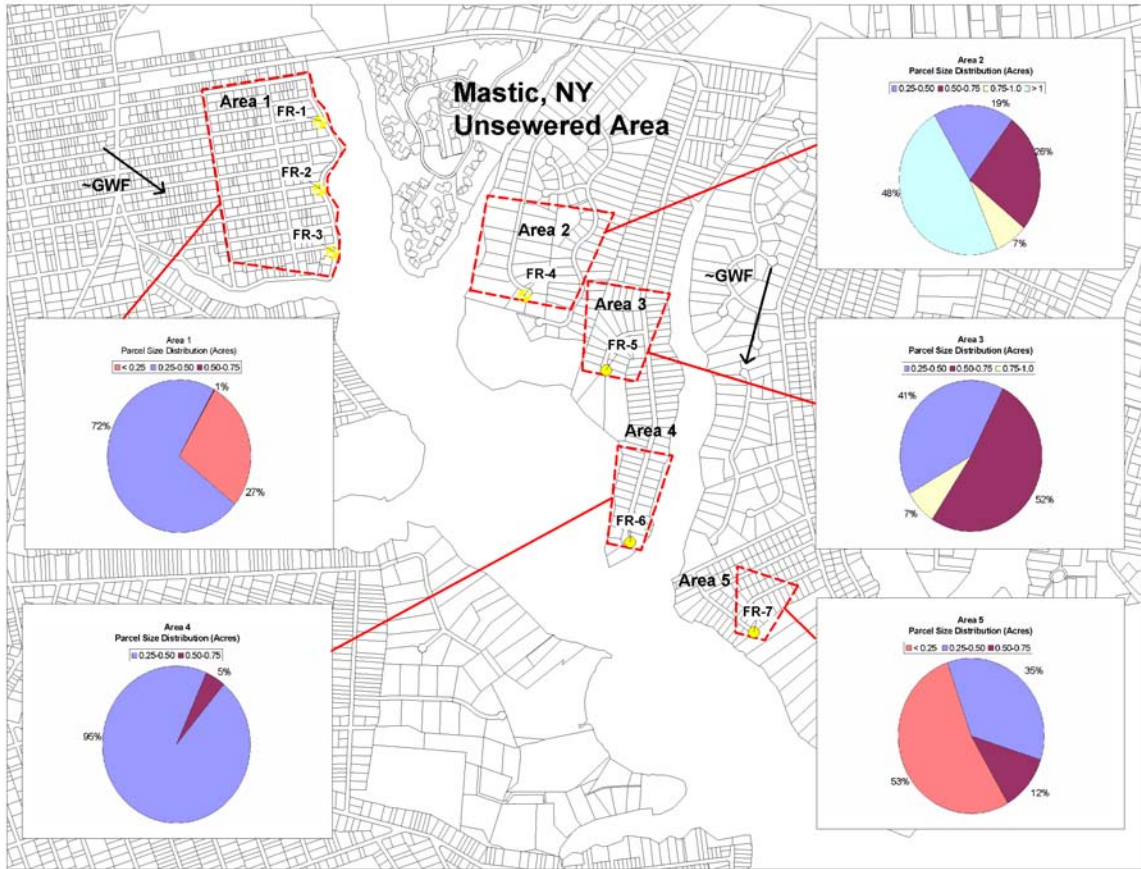


Figure 3-1. Residential density survey

Water quality results from the FR monitoring wells are shown in Table 3-1. Elevated nitrogen levels were detected in monitoring well FR-2, making it an ideal location for a study transect. Water depth and sediment characterization surveys were initially conducted. The water depth survey was recorded during the incoming tide and read a maximum depth of about eight feet in the center of the channel with a gradual decrease towards both shorelines. The sediment characterization survey revealed unconsolidated sediments throughout the FR-

2 transect reaching a maximum depth of about six feet in the middle of the river to almost zero near the shorelines. These initial findings were helpful in determining locations for the *Trident* and *SuperSting* measurements.

Table 3-1. Water quality results for the shoreline wells

Well ID	Sample Date	Latitude	Longitude	Well Depth (fbg)	Screen Depth (fbg)	Conductivity (µS/cm)	Chloride (mg/l)	Ammonia (mg/l)	Nitrite (mg/l)	Nitrate (mg/l)	
FR-1	9/21/2006	40.80052	-72.83192	90	80-85	1500	5	< 0.02	< 0.02	0.3	
				70	60-65	334	57	< 0.02	< 0.02	12.6	
				50	40-45	334	55	1.12	< 0.02	11.4	
				40	30-35	319	50	2.25	< 0.02	9.8	
	9/25/2006			30	20-25	231	51	1.13	< 0.02	8.2	
				20	10-15	230	26	0.02	< 0.02	12.7	
FR-2	4/20/2006	40.79833	-72.83199	95	85-90	368.4	83	< 0.02	< 0.02	0.5	
				75	65-70	284	34	< 0.02	< 0.02	9.1	
				55	45-50	231	28	< 0.02	< 0.02	5.9	
				45	35-40	329.4	44	< 0.02	< 0.02	14.5	
				35	25-30	312.2	42	0.19	< 0.02	10	
				25	15-20	302.6	45	0.56	< 0.02	8.4	
				15	5-10	251.6	44	< 0.02	< 0.02	16.3	
FR-3	4/26/2006	40.79635	-72.83139	120	110-115	31,470	13,532	n/a	n/a	n/a	
				100	90-95	30,320	16,348	n/a	n/a	n/a	
	9/18/2006			80	70-75	28,990	10,764	n/a	n/a	n/a	
				60	50-55	7,400	2,887	0.04	< 0.02	< 0.2	
	9/20/2006			50	40-45	227	48	< 0.02	< 0.02	3.5	
				40	30-35	201	30	< 0.02	< 0.02	2.8	
				30	20-25	281	39	0.47	< 0.02	7.1	
				20	10-15	302	31	5.37	< 0.02	12.5	
				10	0-5	212	34	0.03	< 0.02	0.9	
FR-4	9/25/2006	40.73481	-72.82337	100	90-95	30	11,161	0.43	< 0.02	< 10	
				80	70-75	150	25	< 0.02	< 0.02	0.4	
				60	50-55	68	12	< 0.02	< 0.02	0.5	
	9/26/2006			50	40-45	79	10	< 0.02	< 0.02	0.5	
				40	30-35	68	5	< 0.02	< 0.02	1.5	
					30	20-25	81	8	< 0.02	< 0.02	3.5
					20	39005	175	15	2.02	< 0.02	5.5
FR-5	9/27/2006	40.79251	-72.81985	100	90-95	32,000	14,840	0.49	< 0.02	< 10	
				80	70-75	29,000	13,654	0.72	< 0.02	< 10	
				60	50-55	270	67	0.02	< 0.02	< 0.2	
				50	40-45	160	97	< 0.02	< 0.02	1.6	
	9/28/2006			40	30-35	106	29	< 0.02	< 0.02	1.7	
				30	20-25	69	12	< 0.02	< 0.02	1	
				20	10-15	183	47	< 0.02	< 0.02	1.4	
FR-6	9/28/2006	40.78677	-72.81925	100	90-95	4,730	3,324	0.12	< 0.02	< 10	
				80	70-75	18,600	8,244	0.42	< 0.02	< 10	
	10/2/2006			70	60-65	15,000	6,530	0.27	< 0.02	< 10	
				60	50-55	14,000	6,101	0.25	< 0.02	< 10	
				50	40-45	13,000	5,335	0.23	< 0.02	< 10	
				40	30-35	11,000	4,662	0.2	< 0.02	< 10	
				30	20-25	10,000	4,232	0.18	< 0.02	< 10	
				20	39005	8,000	3,340	0.13	< 0.02	< 10	
FR-7	10/3/2006	40.78400	-72.81405	100	90-95	27,000	12,485	0.76	< 0.02	< 10	
				80	70-75	26,000	12,309	0.71	< 0.02	< 10	
				60	50-55	24,000	10,577	0.81	< 0.02	< 10	
	10/4/2006			50	40-45	19,000	8,031	0.51	< 0.02	< 10	
				40	30-35	500	87	16.1	< 0.02	7.9	
				30	20-25	242	32	4.56	< 0.02	6.1	
				20	39005	154	29	0.07	< 0.02	1.3	

3.1 TRIDENT CONDUCTIVITY AND TEMPERATURE MAPPING

Trident mapping of conductivity and temperature at the groundwater surface water interface was used to identify likely areas of groundwater discharge to the offshore region adjacent to the site. During the summer, Forge River groundwater is colder and has a lower conductivity than the surface water. Thus areas in the sediment having these interstitial water characteristics were identified as likely areas of groundwater discharge. *Trident* mapping locations in the lower Forge River are shown in Figure 3-2. We compiled the data acquired on October 25, 2007 in Table 3-2. The measurements were conducted over a duration of 30 minutes during an incoming tide.



Figure 3-2. Site map showing *Trident* survey locations.

We also present the conductivity data in Figure 3-3. Subsurface conductivities ranged from about 120–16,481 $\mu\text{S}/\text{cm}$, with the lowest values concentrated near station FR2S-2J.



Figure 3-3. Site map showing *Trident* conductivity results for transects FR-2 (conductivity values are in $\mu\text{S}/\text{cm}$).

Table 3-2. Trident results for Forge River transect FR-2

Station ID	Date	Time	Longitude (deg.)	Latitude (deg.)	Push Depth (ft.)	Probe		Reference	
						Average Temperature (°C)	Average Conductivity (µS/cm)	Average Temperature (°C)	Average Conductivity (µS/cm)
FR2S-2A	10/25/2007	11:55	-72.82909	40.79846	1.5	15.6	6,418	17.6	35,385
FR2S-2B	10/25/2007	11:58	-72.82932	40.79847	1.5	18.4	6,421	18.0	36,397
FR2S-2C	10/25/2007	12:01	-72.82956	40.79840	1.5	18.5	13,579	18.4	37,719
FR2S-2D	10/25/2007	12:05	-72.82976	40.79843	1.5	17.9	16,158	18.1	37,674
FR2S-2E	10/25/2007	12:09	-72.83004	40.79838	1.5	18.5	16,481	18.2	38,143
FR2S-2F	10/25/2007	12:12	-72.83033	40.79838	1.5	17.7	11,351	18.3	38,929
FR2S-2G	10/25/2007	12:16	-72.83070	40.79836	1.5	17.5	3,119	18.1	38,929
FR2S-2H	10/25/2007	12:18	-72.83105	40.79835	1.5	16.6	2,524	18.3	38,697
FR2S-2I	10/25/2007	12:21	-72.83142	40.79833	1.5	17.5	1,693	18.1	38,373
FR2S-2J	10/25/2007	12:24	-72.83171	40.79833	1.5	15.9	120	16.9	34,963

The subsurface temperature data are presented in Figure 3-4. Subsurface temperatures in the survey for transect FR-2 ranged from 15.62 to 18.52 °C, with highest temperatures generally found near the middle of the survey area, and colder temperatures closer to the shorelines. Altogether the conductivity and temperature data suggest that SGD near the shores contributed to decreases in bottom parameters. Larger decreases were observed on the west shore, possibly due to stronger discharge of groundwater on this side

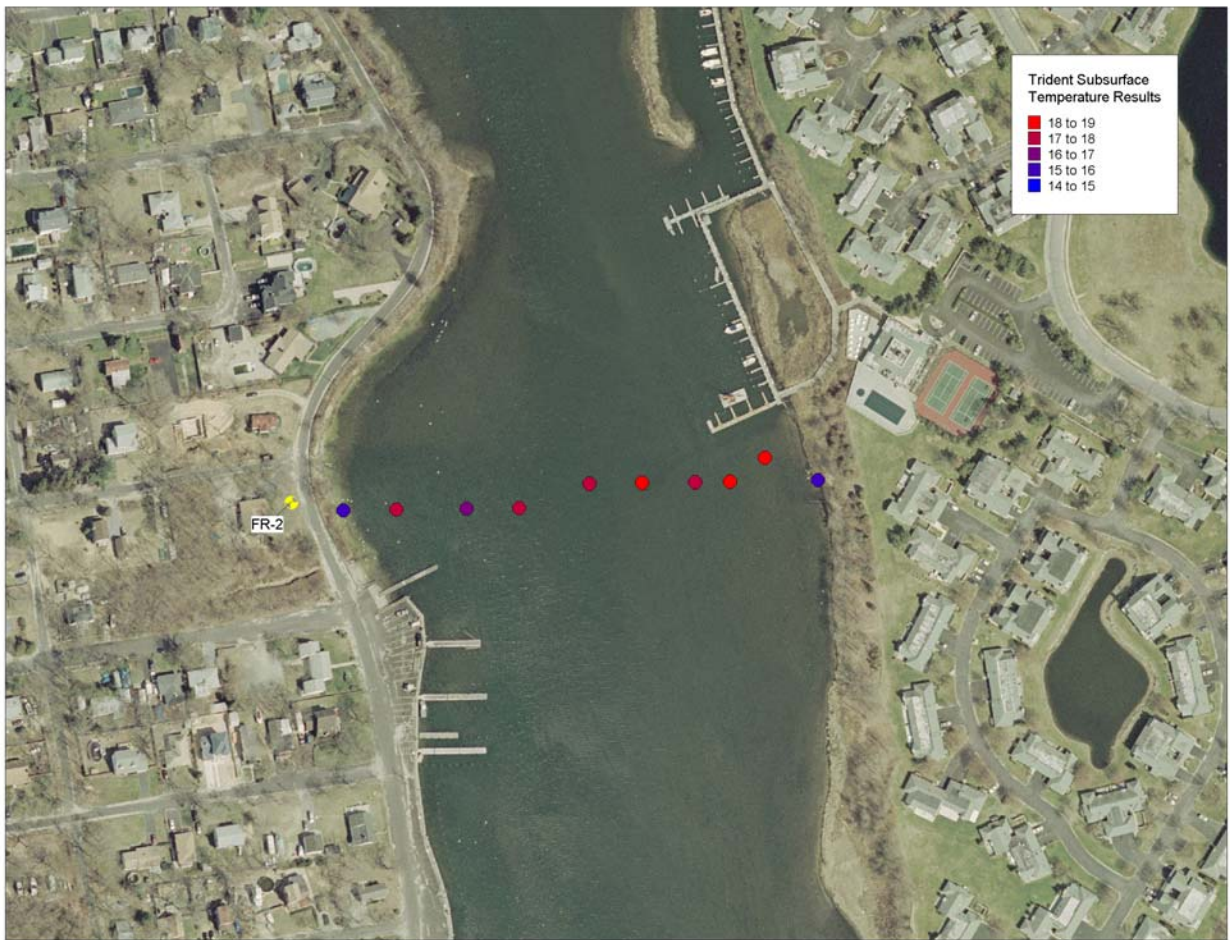


Figure 3-4. Site map showing *Trident* temperature results for transects FR-2 (temperature values are in degrees centigrade).

3.2 SUPERSTING AUTOMATIC RESISTIVITY AND EARTHIMAGER 2D

The *SuperSting* cable was deployed from west to east along transect FR-2. The cable length and electrode spacing are such that the apparent resistivity measured at the sediment surface can be inverted to obtain a resistivity profile down to a depth of approximately 25 feet below the unconsolidated sediment layer of the River. We present in Figure 3-5 the composite of nine profiles that were acquired on August 22, 2007 through August 27, 2007. The hot colors indicate low conductivity and high resistivity, which suggest areas of high groundwater flow. Our data suggest that the strongest SGD near the western shoreline, extended laterally over a distance of several hundred feet. A smaller area of SGD was also observed on the far eastern shoreline. That the west shore is associated with stronger SGD can also be inferred from the *Trident* data, but the *SuperSting* profiling allows us to map out the spatial distribution in detail.

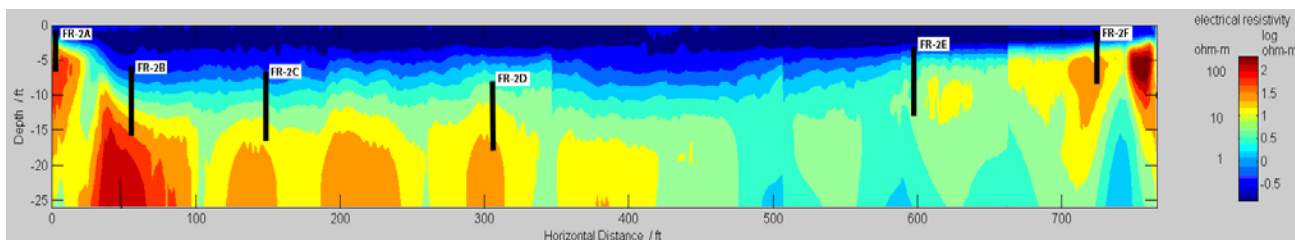


Figure 3-5. SuperSting profile of submarine sediments across transect FR-2 with approximate well-cluster locations and depth

Water depth profiles and underwater terrains were not incorporated into the inversions for Figure 3-5. For comparison, we show in Figure 3-6 a profile that was inverted accounting for the water depth and underwater terrain. The effects are particularly significant near the shores. The data were collected on December 3, 2008 at 10:50 during high tide. The measurement was repeated the same day at 06:50 during low tide (Figure 3-7).

Significant increase in resistivity was observed during low tide, in an area extruding about 50 feet from the shore. The spatial distribution was complex, but there seemed to be two plumes of relatively fresh water: one moved along the sediment surface to a distance of

about 20 feet from the shore and the other was located at a lateral distance of 40 to 50 feet that moved upward in a sub-vertical direction.

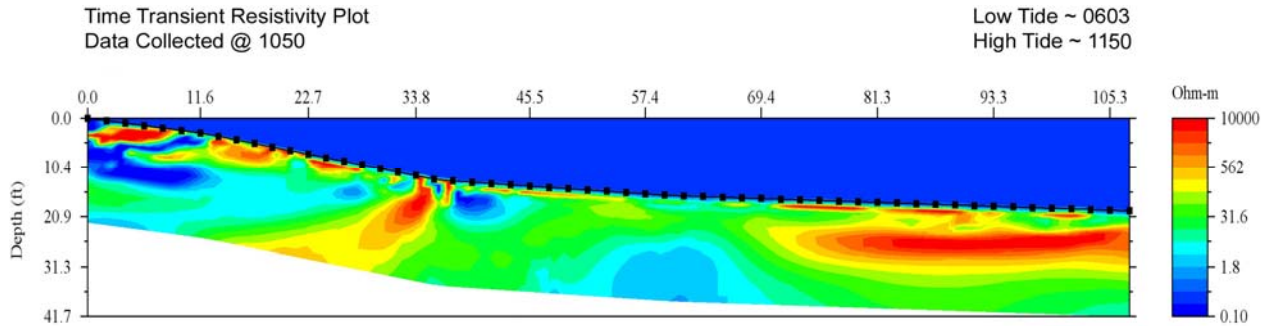


Figure 3-6. Resistivity plot showing little SGD during high tide

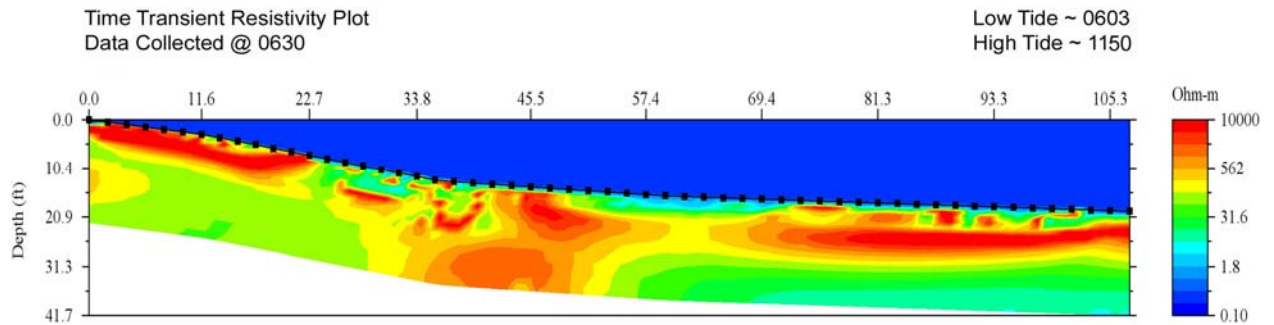


Figure 3-7. Resistivity plot showing increased SGD during low tide

3.3 ULTRASONIC GROUNDWATER SEEPAGE MEASUREMENTS

On the basis of the other data, three stations were selected for Ultrasonic Groundwater Seepage meter deployments (Figure 3-8). At each station two Ultrasonic Groundwater Seepage Meters were deployed at a distance of approximately 20 feet apart. An instrument buoy was connected to the meters and anchored in a central location between the two meters. The meters were left in place for a period of at least one week and the data downloaded from the buoy at the end of the period.



Figure 3-8. Site map showing Ultrasonic seepage meter deployment locations.

FR-2A

Ultrasonic seepage meters were deployed at station FR-2A from October 18 through October 29, 2007. Results for a single 24 hour period at station FR-2A are shown in Figures 3-9 and 3-10. The maximum flow rate for funnel 1 at station FR2-A was 71.51 centimeters per day (cm/d), the minimum was 1.24 cm/d and the average was 48.97 cm/d. For funnel 2 at station FR2-A the maximum flow rate was 103.54 cm/d, the minimum was 0.95 cm/d and the average was 38.93 cm/d. Sediments at this station consist of mostly sand and coarse gravel accounting for relatively high flow rates compared to the two stations further offshore. A rain event occurred on the 19th that could account for high flow throughout the high tide on funnel 1 and the spike in flow rate seen in funnel 2 at station FR2-A.

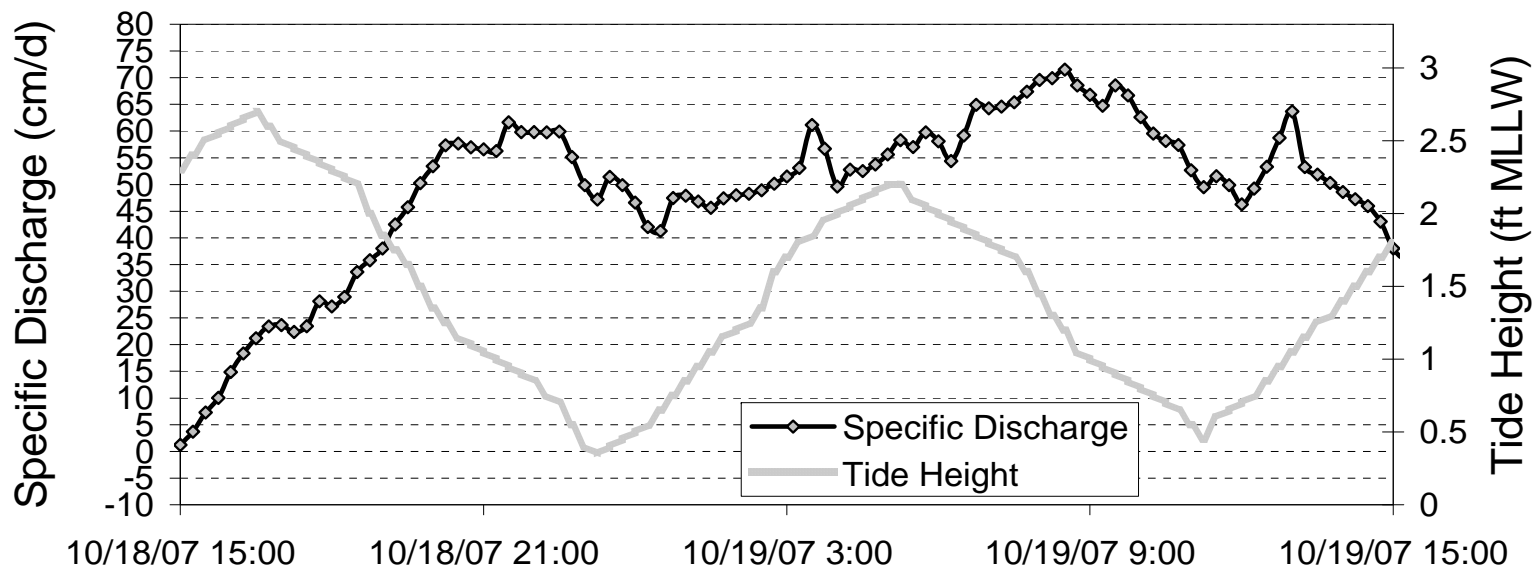


Figure 3-9. Ultrasonic seepage flow data for funnel 1 at Station FR2-A.

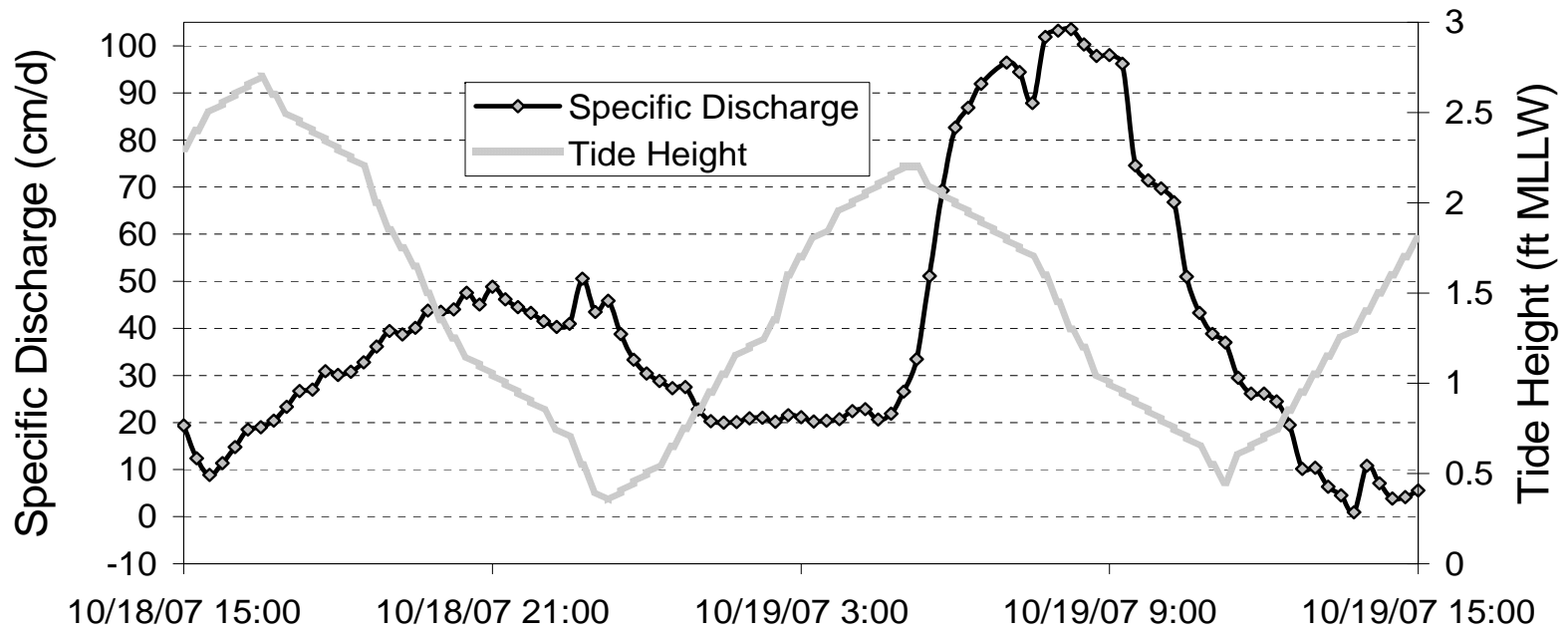


Figure 3-10. Ultrasonic seepage flow data for funnel 2 at Station FR2-A.

FR-2B

Ultrasonic seepage meters were deployed at station FR-2B from October 29 through November 13, 2007. Readings from the flow meter mounted on funnel 2 were erratic and inconsistent during the deployment period and could not be used for flow rate analysis at this location. Results for a single twenty-four hour period for funnel 1 at station FR-2B were plotted and are shown in Figure 3-11. The maximum flow rate for funnel 1 at station FR2-B was 14.88 centimeters per day (cm/d), the minimum was 2.93 cm/d and the average was 7.77 cm/d.

Tidal information is shown for the period showing a slight trend of greater seepage flow during low tides and reduced flow during high tides. The trend is not as pronounced at this site, which could be partly attributed to the thick layer of silt that was present at this location and the lower head pressure caused by the change in gradient.

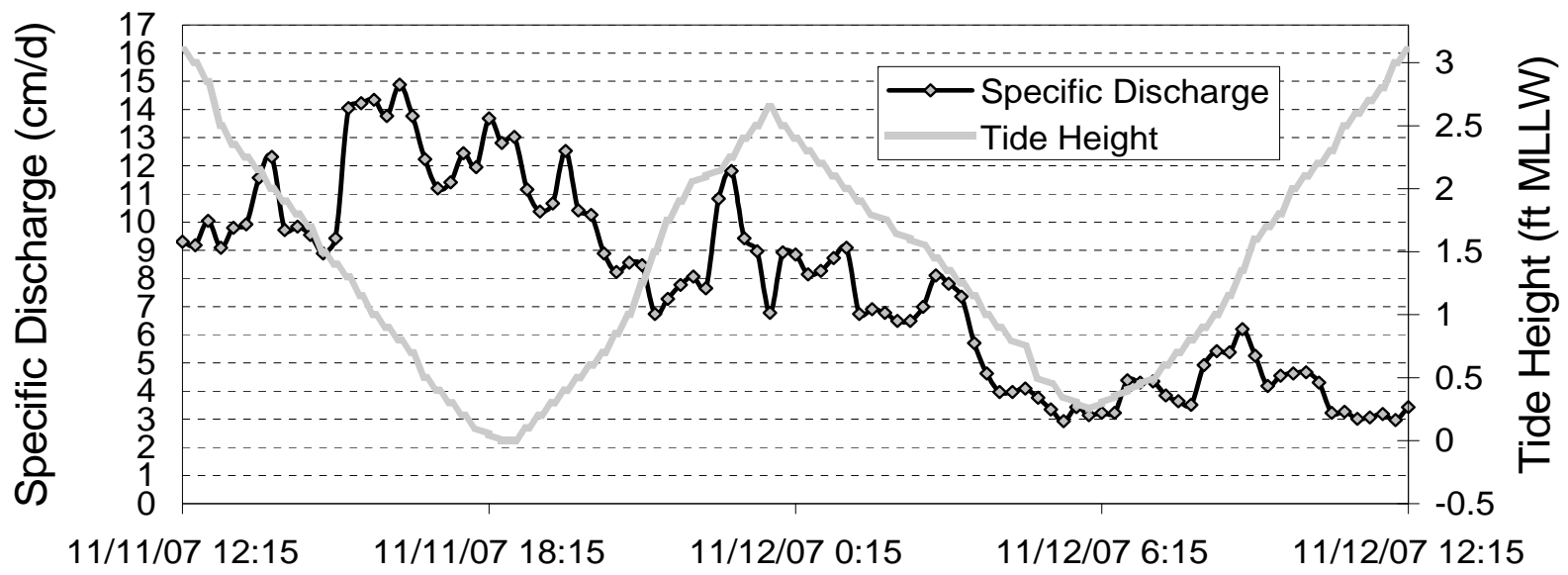


Figure 3-11. Ultrasonic seepage flow data for funnel 1 at Station FR2-B.

FR-2D

Ultrasonic seepage meters were deployed at station FR-2D from November 13 through November 29, 2007. Results for a single twenty-four hour period at station FR-2D were plotted and are shown in Figure 3-12 and 3-13. The maximum flow rate for funnel 1 at station FR2-D-1 was 10.08 centimeters per day (cm/d), the minimum was 0.08 cm/d and the average was 5.39 cm/d. Funnel 2 at station FR2-D-2 had a maximum flow rate of 19.59 cm/d, a minimum flow rate of 12.03 cm/d and an average flow rate of 14.89 cm/d. Station FR-2D is in close proximity to the core sample that had a layer of gravel approximately 12 to 13 feet below the silt layer.

Tidal information is shown for the period indicating a slight trend of greater seepage flow during low tides and reduced flow during high tides. The trend is not as pronounced at this site which could be partly attributed to the thick layer of silt that was present at this location and gradient change.

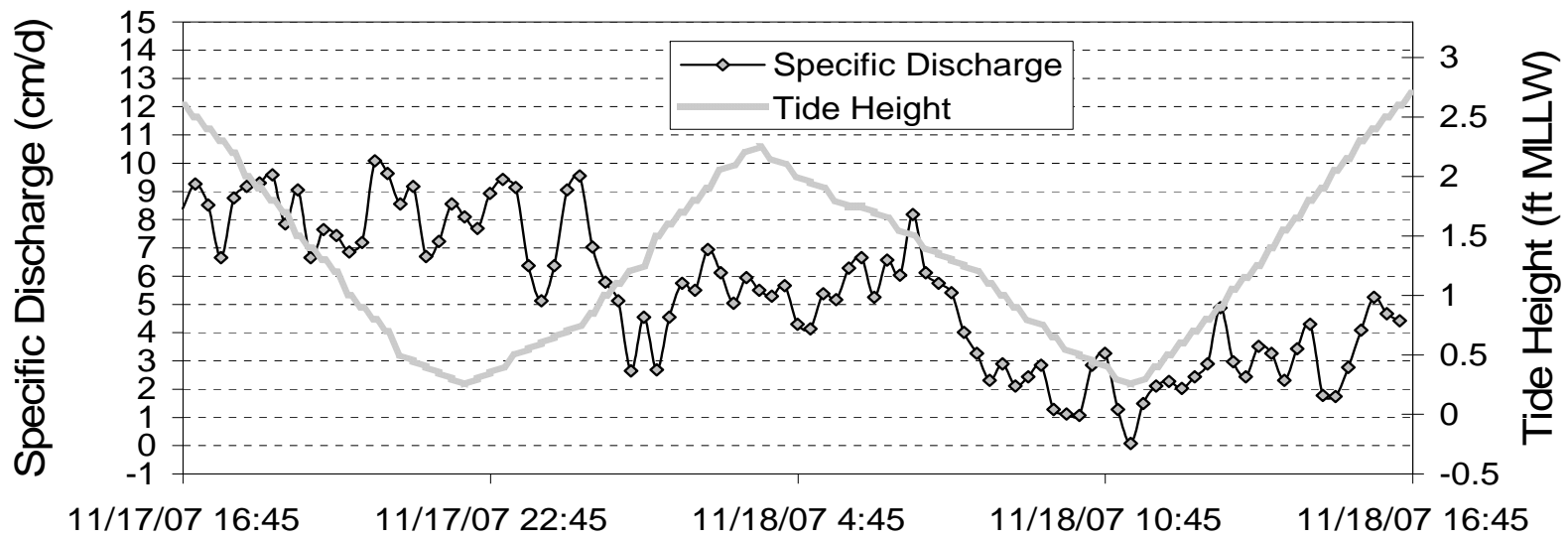


Figure 3-12. Ultrasonic seepage flow data for funnel 1 at Station FR2-D.

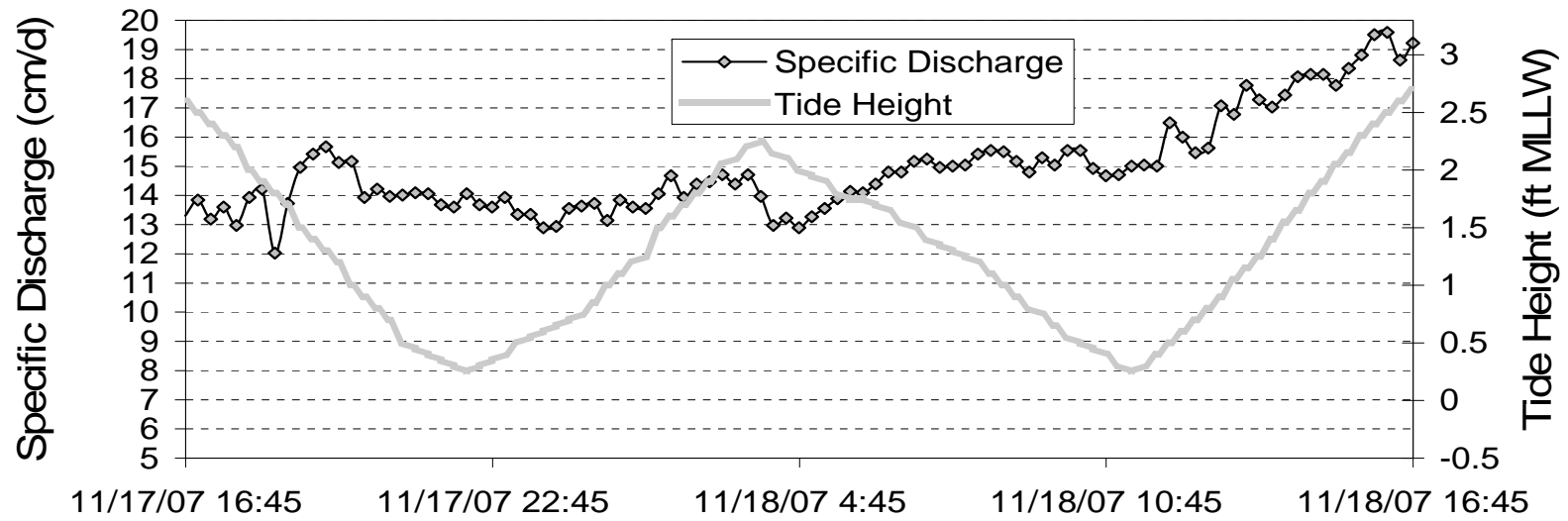


Figure 3-13. Ultrasonic seepage flow data for funnel 2 at Station FR2-D.

3.4 CLUSTER-WELL SURVEY RESULTS

Samples were drawn from the cluster-wells and analyzed at the Suffolk County Public Environmental Health Laboratory (PEHL) for chloride and dissolved metals. FR-2A cluster well on average showed the lowest chloride levels compared to other well clusters. The location of FR-2A is in the intertidal zone on the western shoreline of transect FR-2. Low level chloride was also detected in cluster-well FR-2B. The remaining cluster-wells showed either elevated chloride concentrations or were unable to be processed by the laboratory due to extremely high conductivity or equipment malfunction. High levels of dissolved metals were detected in well FR-2A and FR-2B, the majority of the remaining wells were unable to be sampled due to conductivities that exceeded 2000 $\mu\text{S}/\text{cm}$. The locations of the cluster-wells stations are shown in Figure 3-14. The PEHL laboratory results are shown in Table 3-3. A diagram of the cluster-well locations in relation to the Supersting profile of transect FR-2 is shown in Figure-3-5.



Figure 3-14. Site map showing location of cluster wells.

Table 3-3. Results of cluster well sampling.

Station ID	Latitude	Longitude	Sample Date	Screen Interval (Feet Below Grade)	Field Parameters				Metals		Standard Inorganics (mg/L)			
					Dissolved Oxygen (mg/L)	Temperature (°C)	pH	Conductivity (µS/cm)	Fe (mg/L)	Mn (mg/L)	Chloride	Nitrate	Nitrite	Ammonia
FR-2A (Cluster Well)	40.79837	-72.83183	10/18/07	1-2	1.21	17.8	5.59	368	0.14	705.00	57.0	11.1	< .020	2.31
			10/18/07	2-3	1.08	17.6	5.64	371	0.14	717.00	51.0	11.7	< .020	2.41
			10/18/07	5-6	1.14	17.6	5.70	358	< 0.1	732.00	61.0	8.5	< .020	1.17
			10/23/07	1-2	0.85	17.4	5.42	374	< 0.1	637.00	47.00	10.80	< .020	1.75
FR-2B (Cluster Well)	40.79833	-72.83152	10/18/07	1-2	2.16	20.5	6.26	592	2.63	49.00	140.0	2.3	< .020	0.59
			10/18/07	4-5	2.90	18.7	6.49	217	< 0.1	72.00	28.0	3.2	< .020	< .020
			10/18/07	9-10	2.67	18.8	6.23	283	< 0.1	111.00	45.0	3.4	< .020	< .020
FR-2C (Cluster Well)	40.798833	-72.83125	10/18/07	1-2	2.19	19.1	8.20	4,520	N/A	N/A	956.0	2.8	< .020	0.43
			10/18/07	3-4	2.24	18.4	7.62	460	< 0.1	35.0	81.0	3.3	< .020	0.05
			10/18/07	9-10	9.24	18.6	7.66	25,760	N/A	N/A	8,780.0	3.0	< .020	0.0
			10/23/07	1-2	N/P	21.2	7.53	2,826	N/A	N/A	643.0	1.8	0.03	0.4
FR-2D (Cluster Well)	40.7984	-72.83062	10/23/07	1-2	1.19	21.0	6.40	25,890	N/A	N/A	N/A	N/A	< .020	1.8
			10/23/07	3-4	0.64	20.3	7.13	3,765	N/A	N/A	971.0	< 0.2	< .020	2.2
			10/23/07	9-10	0.89	20.2	6.94	1,898	0.77	285.00	471.0	0.9	< .020	0.1
FR-2E (Cluster Well)	40.79844	-72.82963	10/25/07	2-3	1.45	15.8	6.89	37,980	N/A	N/A	N/A	N/A	< .020	1.7
			10/25/07	5-6	1.55	15.4	6.97	21,310	N/A	N/A	N/A	N/A	< .020	< .020
			10/25/07	9-10	1.32	15.8	6.56	8,344	N/A	N/A	N/A	N/A	< .020	0.2
FR-2F (Cluster Well)	40.79849	-72.82905	10/25/07	0-1	N/A	16.3	5.90	11,670	N/A	N/A	N/A	N/A	< .020	0.11
			10/25/07	2-3	1.20	16.0	6.30	8,665	N/A	N/A	N/A	N/A	< .020	< .020
			10/25/07	6-7	1.85	15.7	5.85	1,499	1.56	55.00	267.0	2.8	< .020	0.02
FR-2 (Surface Water)	-	-	10/18/07	-	6.27	17.6	6.31	37,800	N/A	N/A	14,500.0	4.7	< .020	0.23
	40.7984	-72.83062	10/23/07	-	3.22	20.1	6.23	32,840	N/A	N/A	N/A	N/A	< .020	0.31

3.5 CORE SAMPLING RESULTS

Sediment core samples were collected at selected locations along transect FR2. The results of the core sampling show that the sediments below the silty muck layer consist of mostly fine to medium sand. At one location (FR-2C-D) a layer of gravel is present approximately 12 to 13 feet below the river bottom. The location of the core sampling is shown in Figure 3-15.



Figure 3-15. Site map showing location of sediment core sampling.

Table 3-4. Core sample classification for transect FR-2.

Site ID	Coring Depth (Below River Bottom)	Description
FR-2C-D	5'-9'	Fine to Medium Grayish Brown Sand with some coarse sand and fine gravel
	9'-13'	Well sorted Fine to Medium Light Brown Sand with some coarse sand 11'-12'; Fine to Coarse Gravel 12'-13'
	13'-17'	Fine to Medium Light Brown to Brown sand with some coarse sand
FR-2C-G	4'-8'	Fine to Medium Grayish Brown Sand with some coarse sand
	8'-12'	Fine to Medium Light Brown Sand with some coarse sand
	12'-16'	Fine to Medium Light Brown to Brown Sand with some coarse sand and few fine gravel
FR-2C-H	6'-10'	Fine to Medium Brown Sand with fine to coarse gravel
	10'-14'	Fine to Medium Light Brown to Brown Sand with some coarse sand and fine gravel
	14'-18'	Fine to Medium Brown Sand with some coarse sand and silt

*The upper portion of the sediments at each of the core sample locations consists of a silty layer that was too loose to recover as a core sample.

4 CONCLUSIONS

4.1 CONCLUSIONS

Based on the data that was collected, the following conclusions have been reached. The *Trident* sampling system was able to distinguish and map the spatial distribution of low conductivity areas which indicate possible SGD. These areas were concentrated around the shorelines, with the strongest SGD signal occurring on the western shore. This is most likely attributed to the greater relief of the onshore terrain, which would cause a larger hydraulic gradient, thus increasing the amount of SGD compared to the eastern shore. One of the main drawbacks of the *Trident* system is the inability to collect data points at a depth greater than three feet. Areas that have deeper SGD pockets will be undiscovered if the *Trident* system was the only tool being used.

The *SuperSting* Resistivity system, which is also able to characterize the spatial distribution of SGD, does not have the same limiting depth factor as the *Trident* system and therefore will be able to delineate deeper SGD pockets. The *SuperSting* system also has the ability to determine temporal distribution of SGD. The results over a tide cycle showed the increased movement of SGD through the underlying sediments during the period of a high to low tide. The increased SGD movement indicates that tidal fluctuations play a major role in the discharge rate of submarine groundwater. One disadvantage when using the *SuperSting* system for a time transient event is the fact that the system needs to be restarted after each test period. This limits the amount of data that can be collected due to time restraints and availability of field personnel.

The ultrasonic seepage meter, though very site specific can be deployed easily and left over a longer period with little interaction required from field personnel. The data recorded from the ultrasonic seepage meter gives you the ability to compare specific discharge rates with tide fluctuations and even rain events.

During this study, six cluster wells were installed and sub-surface samples were collected. These samples were used for data validation against the techniques previously described. By comparing the results from the shallow levels of the cluster wells, we are able to see that the *Trident* conductivities and well samples both show a fresh water signal near shore and a much weaker to non-existent signal towards the center of the river. This positive comparison proves that the *Trident* is a useful and

effective tool when conducting a multi point survey. By comparing the water chemistry against the *SuperSting* resistivity results we are able to see that the *SuperSting* has the ability to detect and map freshwater pockets in the sub-surface sediments. We are also able to conclude that the *SuperSting* is measuring the resistivity of the pore fluids and not the electrical resistivity of the porous medium.

The different techniques used in this study to detect SGD have been proven effective. Each piece of equipment has been specially designed to complete a certain task. By using a single device one can only see part of the picture. In order to create a clear and concise understanding of how SGD enters a body of water, an in-depth survey needs to be completed using all of the equipment described.

5 REFERENCES

- Aller, R. C., C. J. Gobler, and B. J. Brownawell (2009), Data report on benthic flux studies and the effect of organic matter remineralization in sediments on nitrogen and oxygen cycling in the Forge River, New York; Task #1 and 2, Prepared for Suffolk County Department of Health Services, 62 pp, School of Marine and Atmospheric Sciences, Stony Brook University, Stony Brook.
- Bokuniewicz, H. J., and M. J. Zeitlin (1990), Characteristics of the Ground-Water Seepage Into Great South Bay, 32 pp, Marine Sciences Research Center, State University of New York, Stony Brook.
- Chadwick, D. B., A. Gordon, J. Groves, C. Smith, R. Paulsen, and B. Harre (2003), New tools for monitoring coastal contaminant migration, *Sea Technology*, 17-22.
- Day-Lewis, F. D., E. A. White, C. D. Johnson, J. W. J. Lane, and M. Belaval (2006), Continuous resistivity profiling to delineate submarine groundwater discharge - examples and limitations, *The Leading Edge*, 724-728.
- Mao, X., P. Enot, et al. (2006), Tidal influence on behaviour of a coastal aquifer adjacent to a low-relief estuary, *Journal of Hydrology*, 327, 110-127.
- Martin, J. B., J. E. Cable, et al. (2007), Magnitudes of submarine groundwater discharge from marine and terrestrial sources: Indian River Lagoon, Florida. *Water Resources Research*, 43.
- Paulsen, R. J., C. F. Smith, D. O'Rourke, and T.-f. Wong (2001), Development and evaluation of an ultrasonic ground water seepage meter, *Ground Water*, 39, 904-911.
- Paulsen, R. J., D. O'Rourke, C. F. Smith, and T.-f. Wong (2004), Tidal load and saltwater influences on submarine ground water discharge, *Ground Water*, 42, 990-999.

- Swarzenski, P. W., F. W. Simons, A. J. Paulson, S. Kruse, and C. Reich (2007), Geochemical and geophysical examination of submarine groundwater discharge and associated nutrient loading estimates into Lynch Cove, Hood Canal, WA, *Eng. Sci. Tech.*, *41*, 7022-7029.
- Taniguchi, M. (2002), Tidal effects on submarine groundwater discharge into the ocean, *Geophys. Res. Lett.*, *29*, 2-1, 10.1029/2002GL014987.
- Taniguchi, M., T. Ishitobi, and J. Shimada (2006), Dynamics of submarine groundwater discharge and freshwater-seawater interface, *J. Geophys. Res.*, *111*, C01008, doi:10.1029/2005JC002924.
- Telford, W. M., L. Geldart, and R. E. Sheriff (1990), *Applied Geophysics*, 2nd ed., 770 pp., Cambridge University Press, Cambridge.
- Zektser, I. S., L. G. Everett, and R. G. Dzhamaalov (2006), *Submarine Groundwater*, 466 pp., CRC Press, Boca Raton, FL.